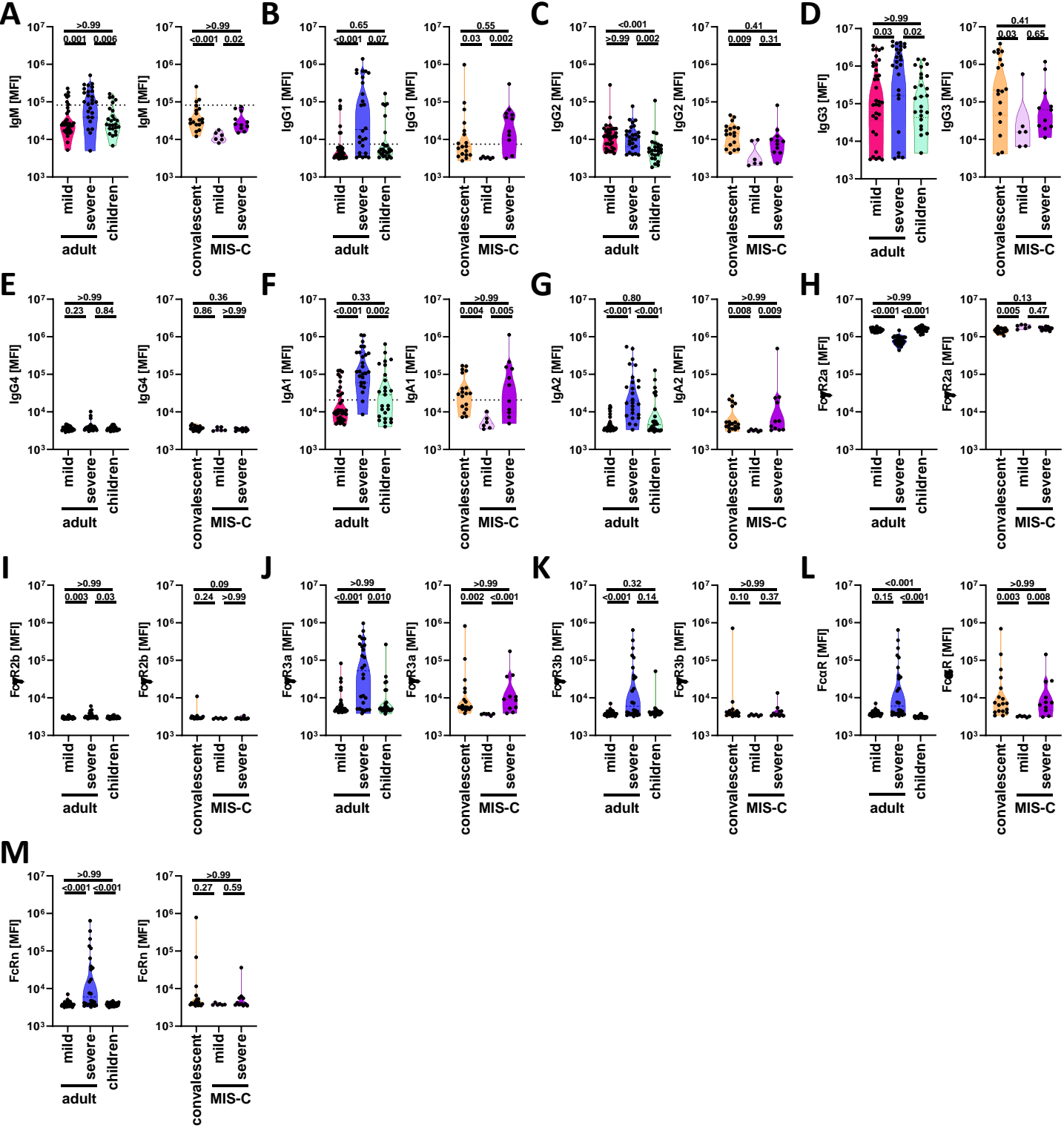
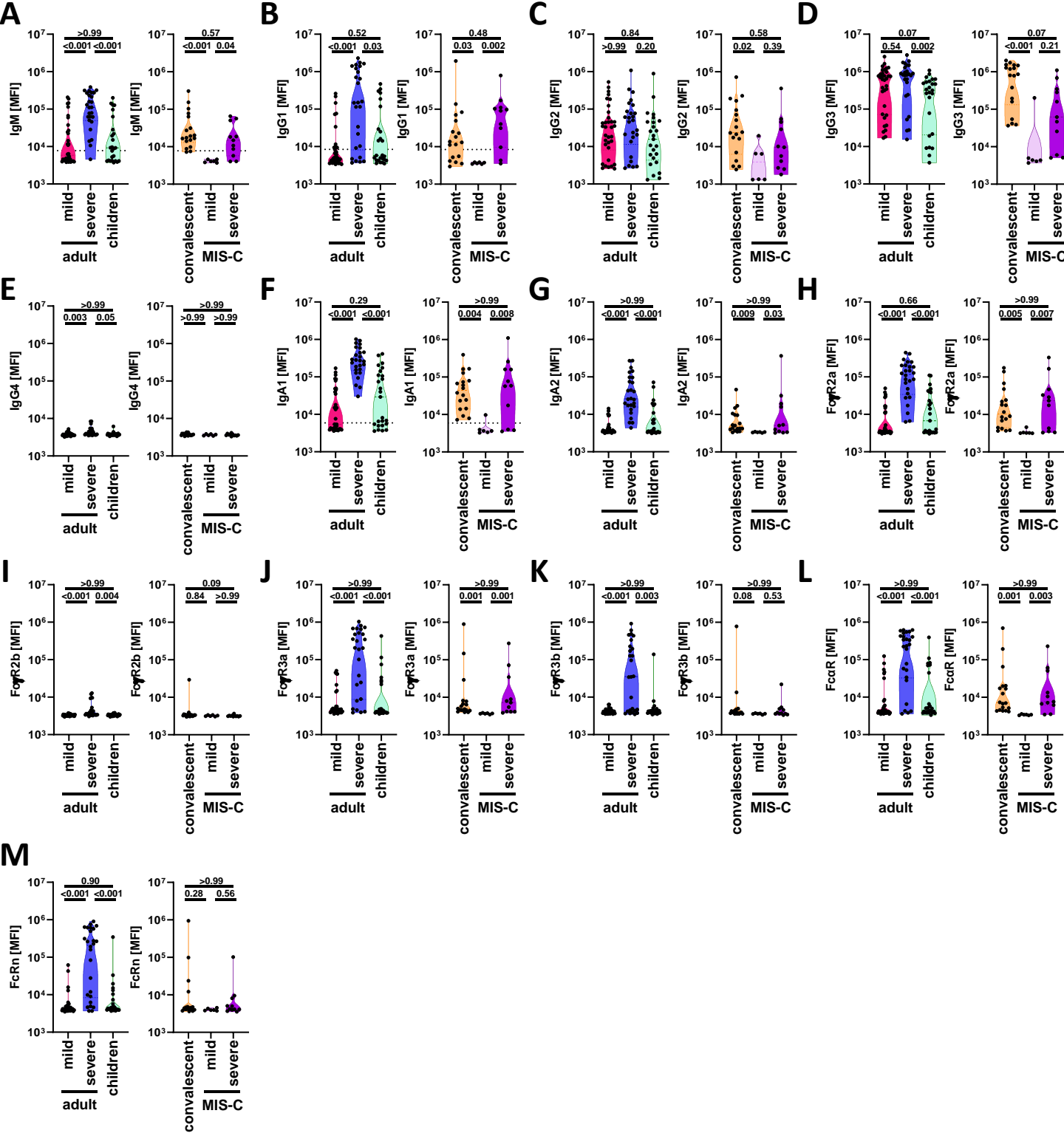

Supplementary information

Humoral signatures of protective and pathological SARS-CoV-2 infection in children

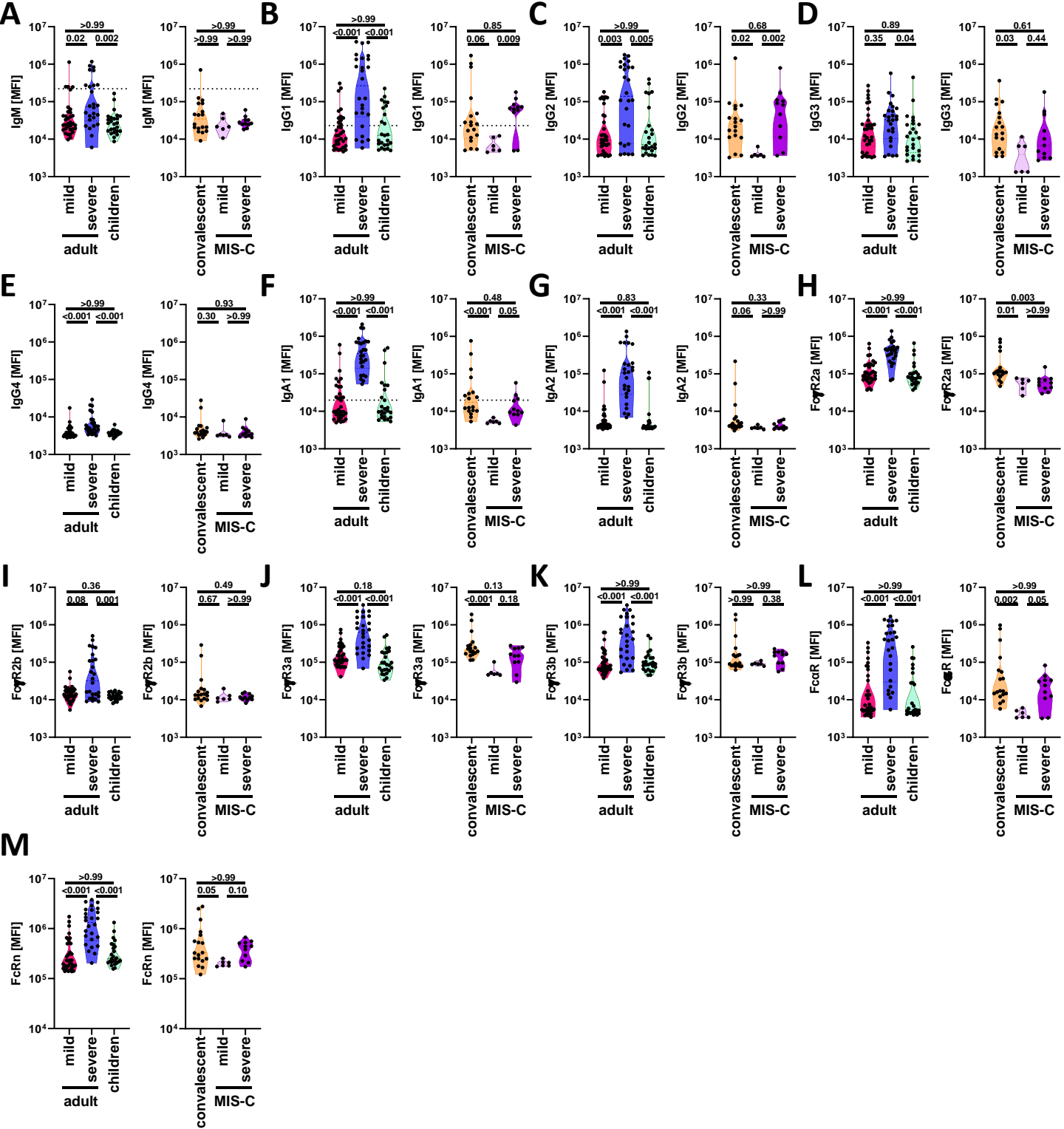
In the format provided by the authors and unedited



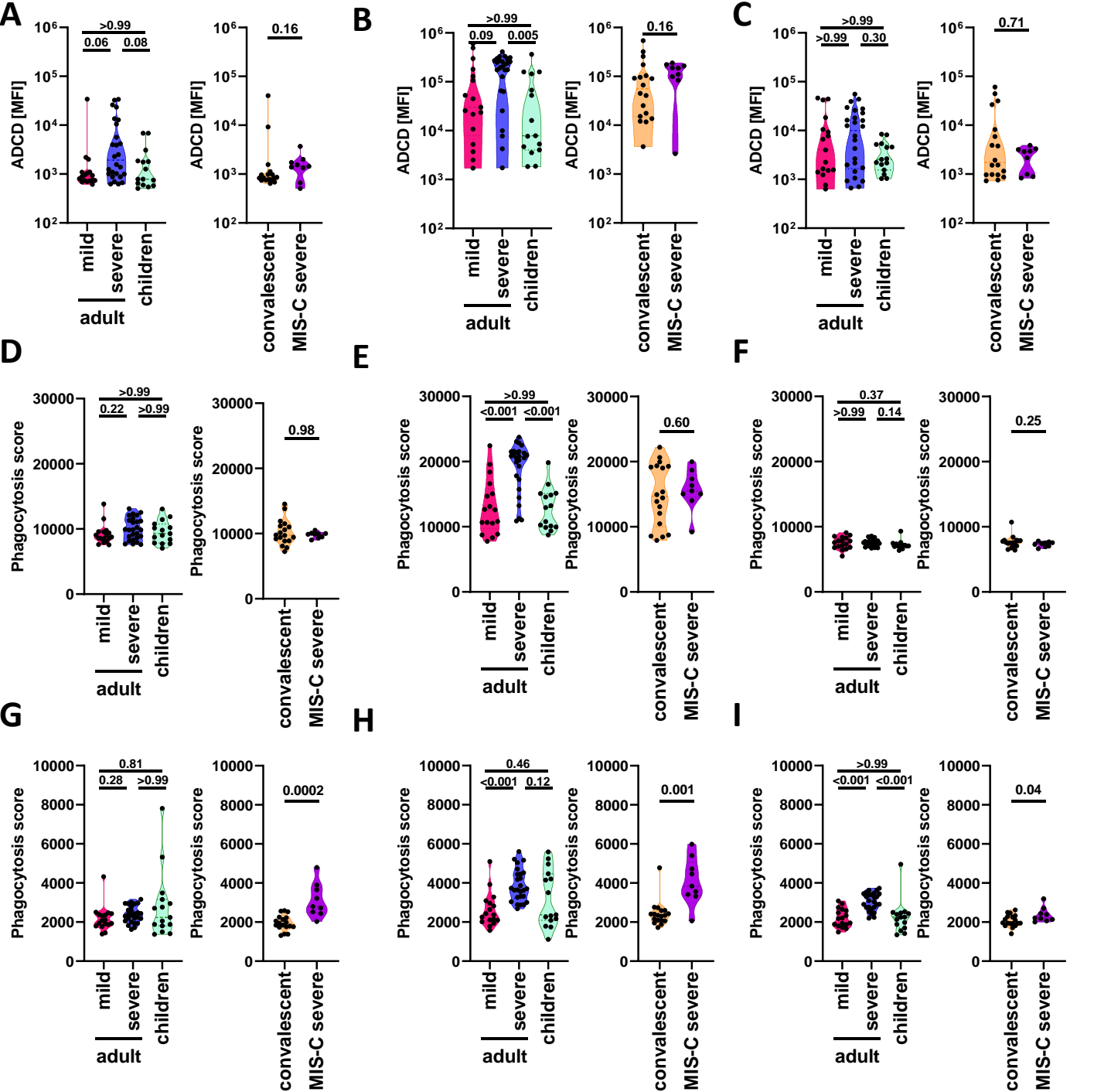
Supplemental Figure 1: Analysis of SARS-CoV-2 RBD specific IgM (A), IgG1 (B), IgG2 (C), IgG3 (D), IgG4 (E), IgA1 (F), IgA2 (G), FcγR2a (H), FcγR2b (I), FcγR3a (J), FcγR3b (K), FcαR (L) and FcRn (M) ($n_{\text{mild}}=34$, $n_{\text{severe}}=26$, $n_{\text{SARS+ children}}=25$, $n_{\text{mild_MIS-C}}=6$, $n_{\text{severe_MIS-C}}=11$, $n_{\text{convalescent}}=18$). The dotted line represents the average plus 5 times the standard deviation of the negative plasma samples used to determine seropositivity (see Methods). A non-parametric Kruskal-Wallis test was used to test for statistically significant differences between multiple groups. These data were also compiled in flower plots in Figure 1 and 4.



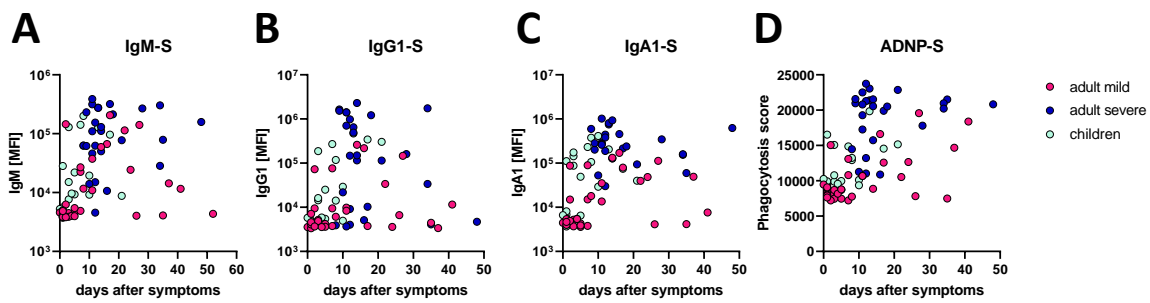
Supplemental Figure 2: Analysis of SARS-CoV-2 S specific IgM (A), IgG1 (B), IgG2 (C), IgG3 (D), IgG4 (E), IgA1 (F), IgA2 (G), FcγR2a (H), FcγR2b (I), FcγR3a (J), FcγR3b (K), FcαR (L) and FcRn (M) ($n_{\text{mild}}=34$, $n_{\text{severe}}=26$, $n_{\text{SARS+ children}}=25$, $n_{\text{mild_MIS-C}}=6$, $n_{\text{severe_MIS-C}}=11$, $n_{\text{convalescent}}=18$). The dotted line represents the average plus 5 times the standard deviation of the negative plasma samples used to determine seropositivity (see Methods). A non-parametric Kruskal-Wallis test was used to test for statistically significant differences between multiple groups. These data were also compiled in flower plots in Figure 1 and 4. Additionally, graphs in A, B and F are also shown in Figures 1 or 4.



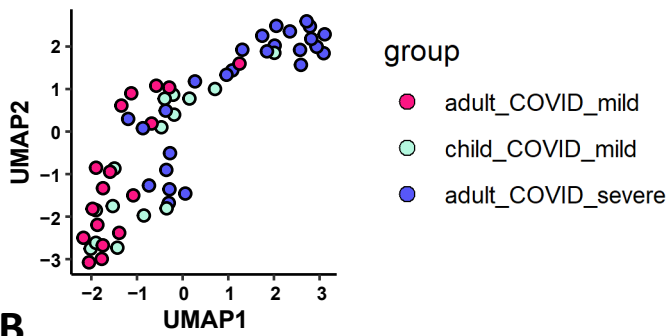
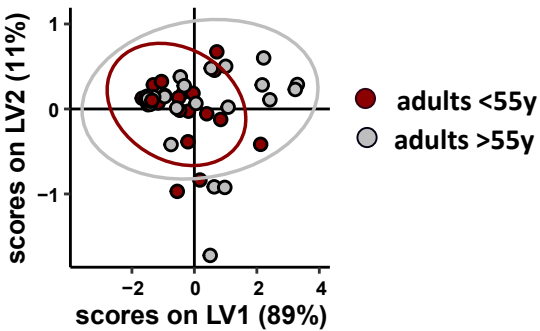
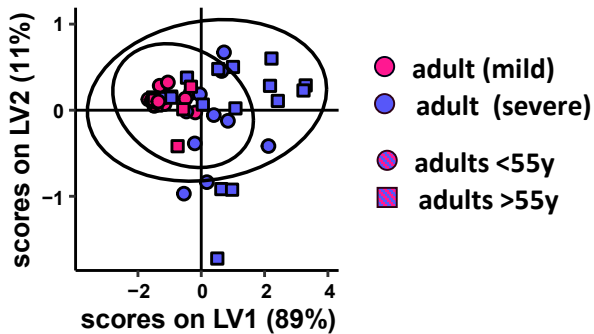
Supplemental Figure 3: Analysis of SARS-CoV-2 N specific IgM (A), IgG1 (B), IgG2 (C), IgG3 (D), IgG4 (E), IgA1 (F), IgA2 (G), FcγR2a (H), FcγR2b (I), FcγR3a (J), FcγR3b (K), FcαR (L) and FcRn (M) ($n_{\text{mild}}=34$, $n_{\text{severe}}=26$, $n_{\text{SARS+ children}}=25$, $n_{\text{mild MIS-C}}=6$, $n_{\text{severe MIS-C}}=11$, $n_{\text{convalescent}}=18$). The dotted line represents the average plus 5 times the standard deviation of the negative plasma samples used to determine seropositivity (see Methods). A non-parametric Kruskal-Wallis test was used to test for statistically significant differences between multiple groups. These data have also been included as flower plots in Figure 1 and 4.



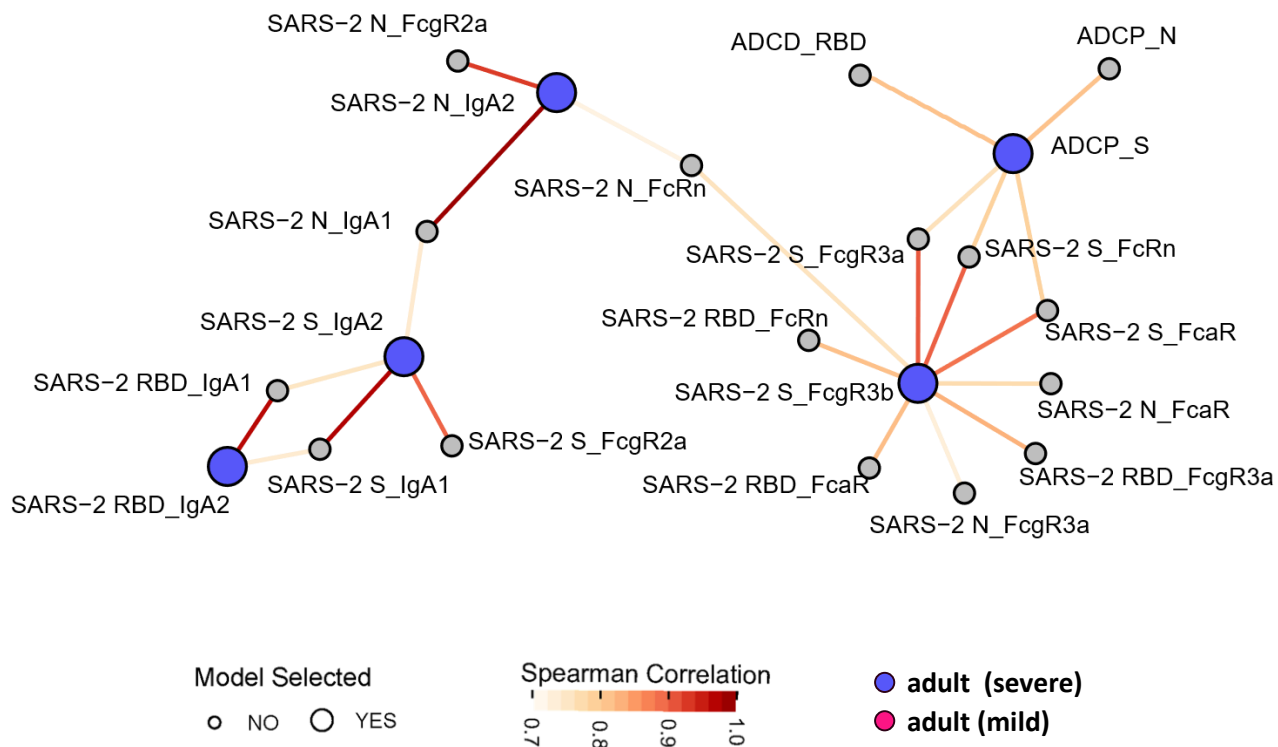
Supplemental Figure 4: SARS-CoV-2 RBD (A), S (B) and N (C) specific antibody-dependent complement deposition (ADCD). SARS-CoV-2 RBD (D), S (E) and N (F) specific antibody-dependent neutrophil phagocytosis (ADNP) and SARS-CoV-2 RBD (G), S (H) and N (I) specific antibody-dependent monocyte phagocytosis (ADCP) were assessed across $n_{\text{mild adults}}=17$, $n_{\text{severe adults}}=26$, $n_{\text{children}}=15$, $n_{\text{conv}}=18$, $n_{\text{severe MIS-C}}=9$. A non-parametric Kruskal-Wallis test was used to test for statistically significant differences between multiple groups and two-sided Mann-Whitney test was used to test for statistically significant differences between the two groups. These data have also been included as flower plots in Figure 1 and 4. Additionally, graphs in B, E and H are also shown in Figures 1 or 4.



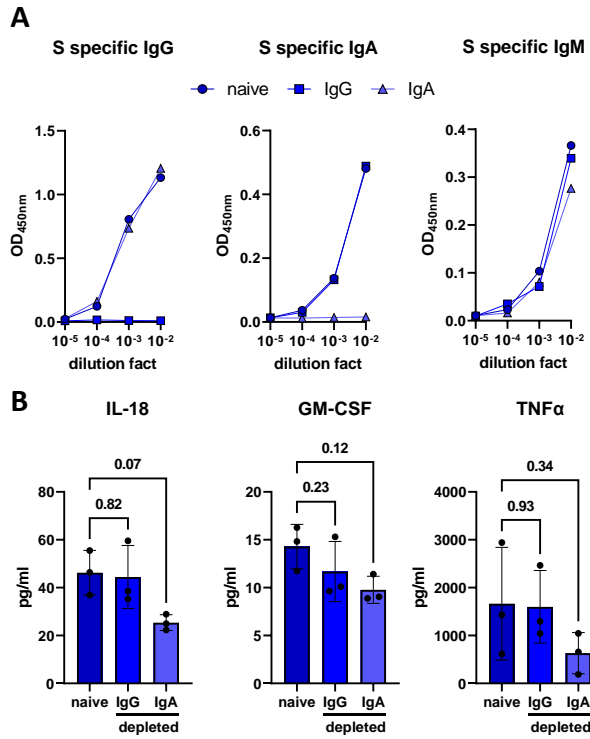
Supplemental Figure 5: Time dependency of SARS-CoV-2 specific antibody responses in acute disease. IgM (A), IgG1 (B), IgA1 (C) and ADNP (D) responses against SARS-CoV-2 S are shown for mildly ill children, adults with mild disease, or severely ill adults from the day of symptom onset.

A**B****C**

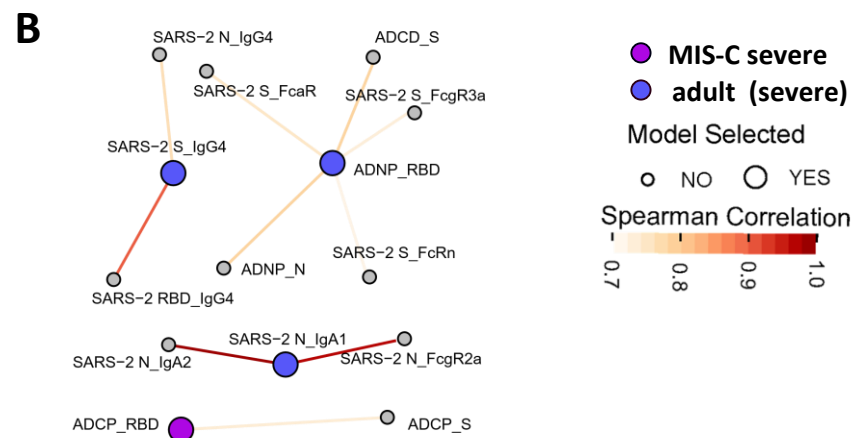
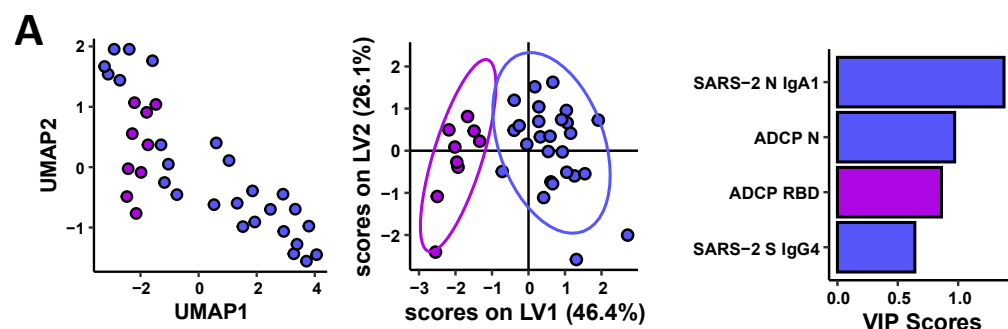
Supplemental Figure 6: A) A three-way UMAP analysis shows the comparison of the multivariate SARS-CoV-2-specific humoral response across severely ill adults, mildly ill adults, and children. B) The LASSO/PLS-DA analysis shows the comparison of SARS-CoV-2 specific antibody profiles across age-groups, split along a median age split (55 years). The model was not significant (cross-validation accuracy: 0.5895). C) Instead, the same LASSO/PLS-DA as in B) was colored by disease severity (mild or severe), age is indicated by symbol, demonstrating better separation.



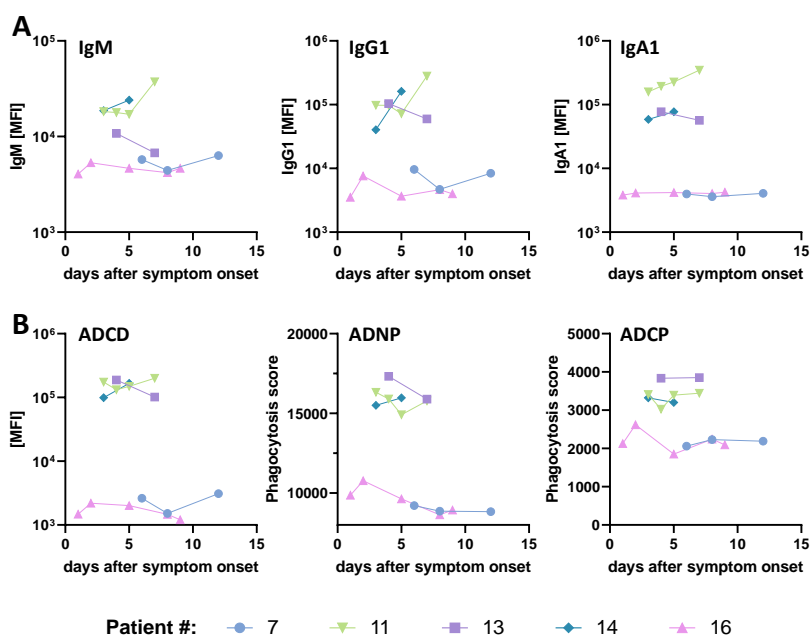
Supplemental Figure 7: The Correlation network shows the analysis of LASSO selected (big circles) or non-selected (small circles) features that were selectively enriched across mild and severely ill adults. Connections between points (features) indicate significant ($p > 0.05$) Spearman correlations. Fill colors of the circles indicate the specific group in which the selected feature was enriched (grey = feature was not selected), the color of connecting lines indicates the correlation coefficient (compare Figure 2).



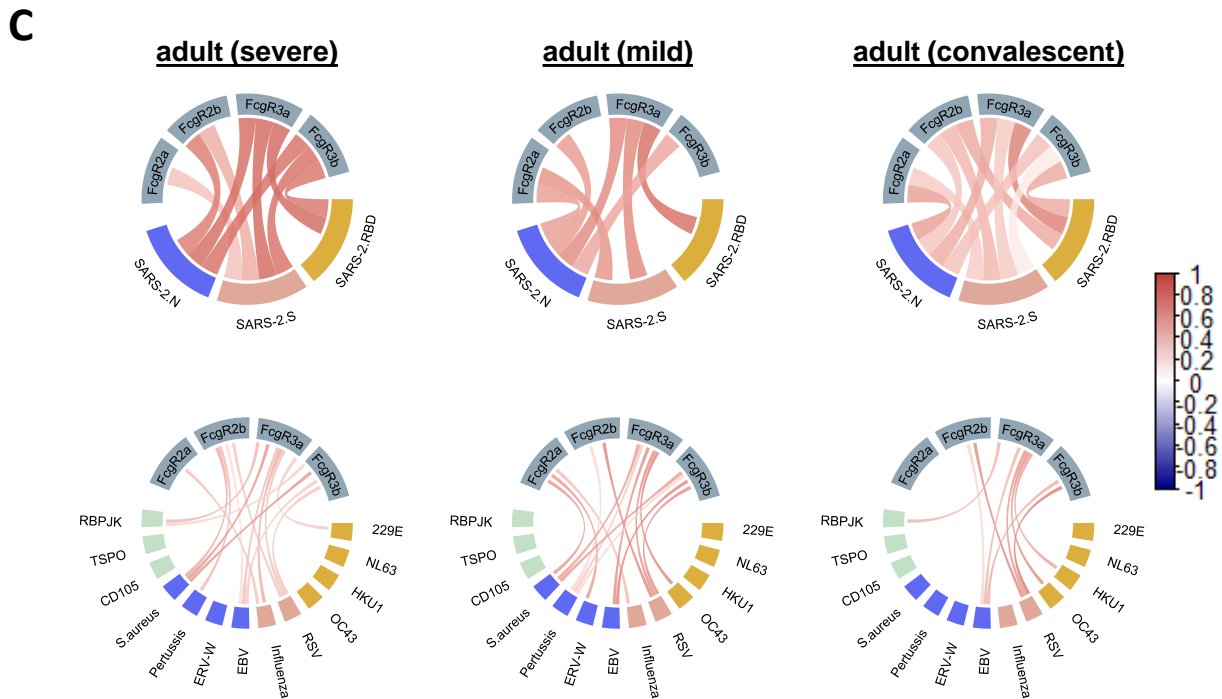
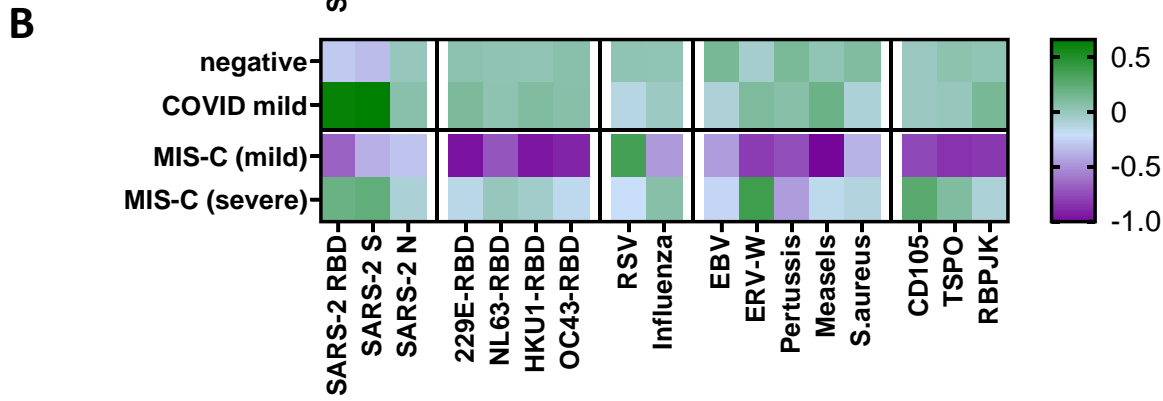
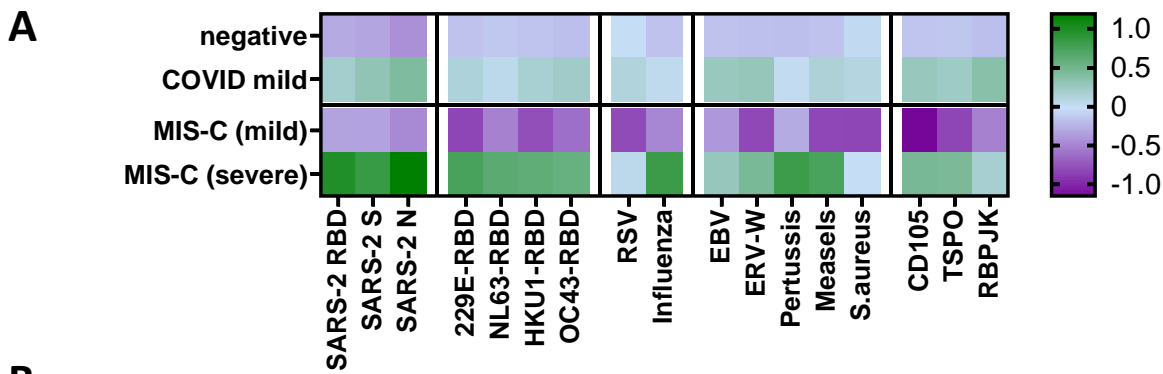
Supplemental Figure 8: Plasma samples from severely ill adult COVID19 patients were pooled and IgA and/or IgG were subsequently depleted. (A) The line graph confirms the isotype specific depletion of S-specific antibodies in the individual pools by S-specific IgG, IgA and IgM ELISA (data from one experiment is shown). (B) The graph indicates the primary neutrophil derived cytokine secretion profiles across three healthy donors following a 4 hour stimulation with SARS-CoV-2 S specific immune complexes. The release of IL-18, GM-CSF and TNF α were determined by multiplex cytokine Luminex. Data are presented as mean values +/- SD of three individual blood neutrophil donors.



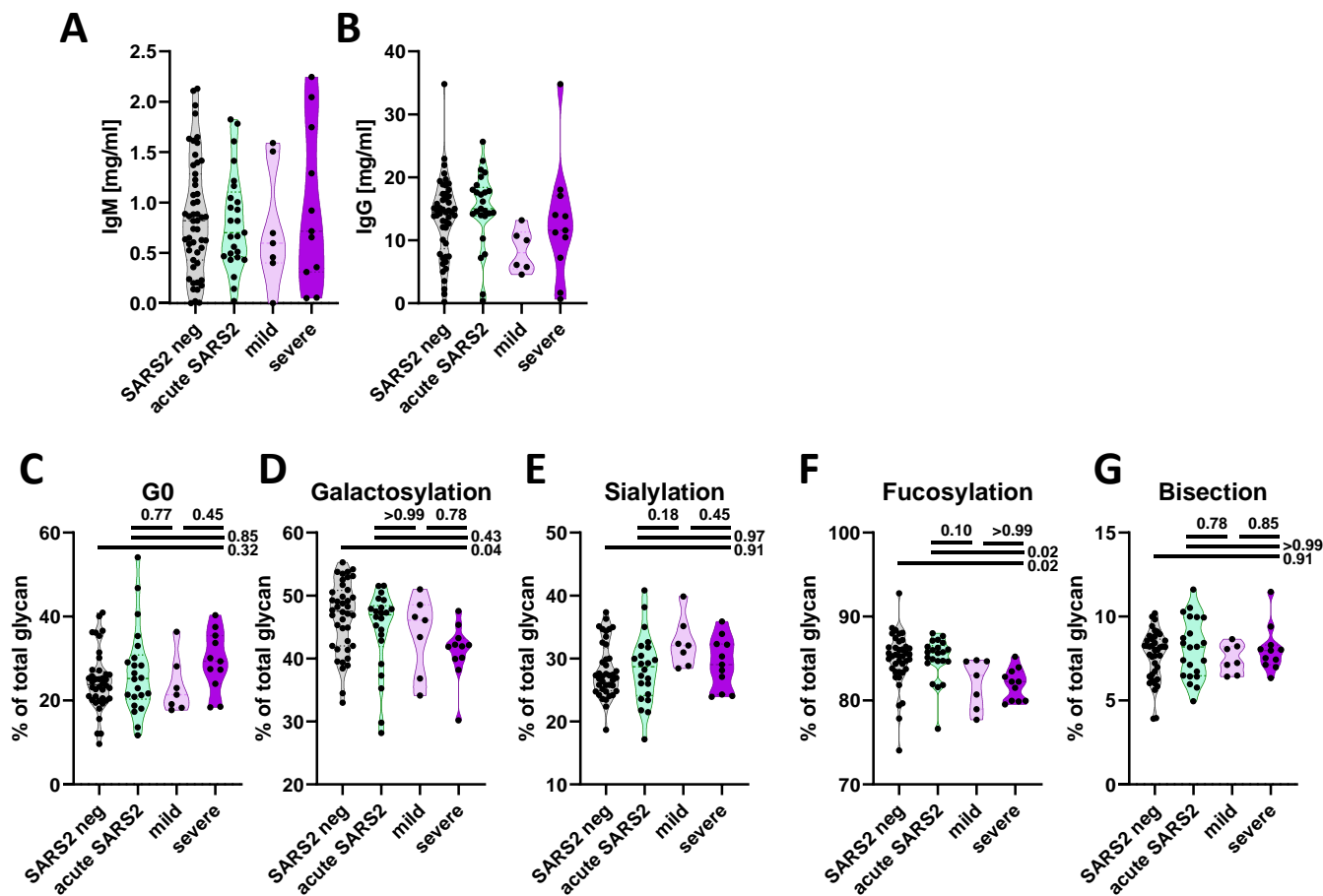
Supplemental Figure 9: (A) Pairwise comparisons by UMAP and LASSO/PLS-DA analyses are shown for children with severe MIS-C and severe acutely infected adults ($n_{\text{severe MIS-C}}=9$, $n_{\text{severe-adults}}=26$) with a cross-validation accuracy of 0.99. B) The correlation network of LASSO selected (big circles) or unselected (small circles) features are shown across children and severely ill adults. Connection between points (features) indicate significant relationships ($p>0.05$) defined by a Spearman correlation after Benjamini-Hochberg correction. Fill color of the circles indicate in which group the selected feature were enriched (grey = feature was not selected), the color of connecting lines indicate the correlation coefficient.



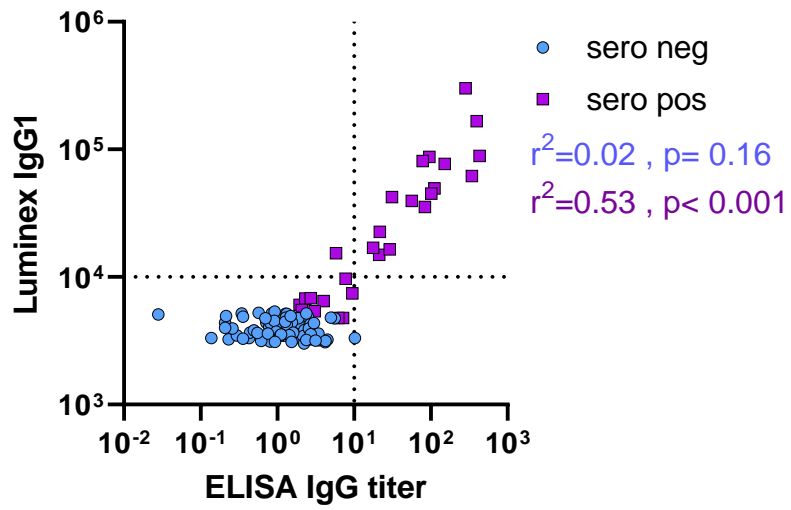
Supplemental Figure 10: (A) The graph shows the time course of the S-specific humoral IgM, IgG1 and IgA1 titers and (B) ADCD, ADNP and ADCP functions in five severe MIS-C patients (compare Patients # with Supplemental Table 2).



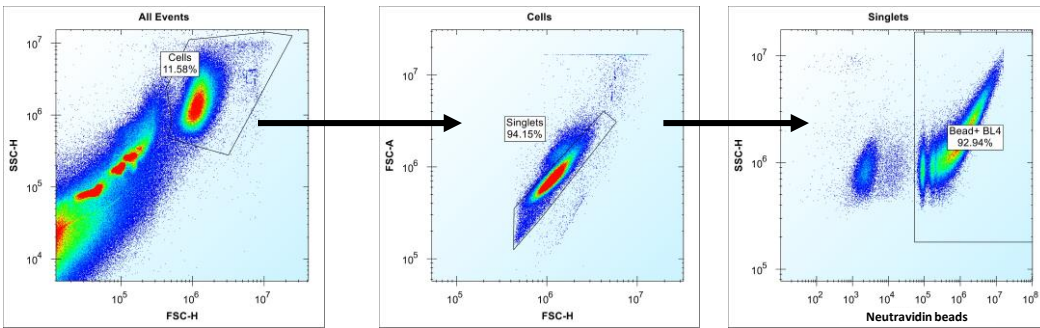
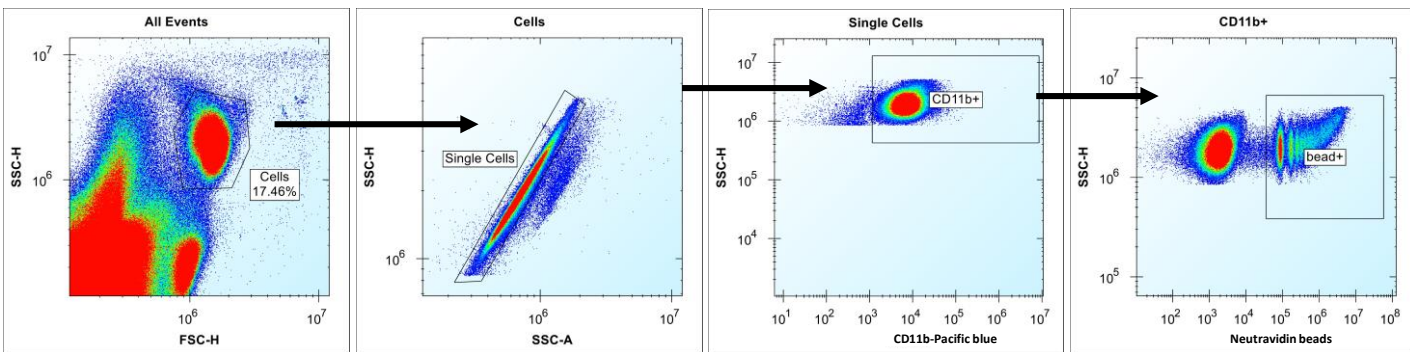
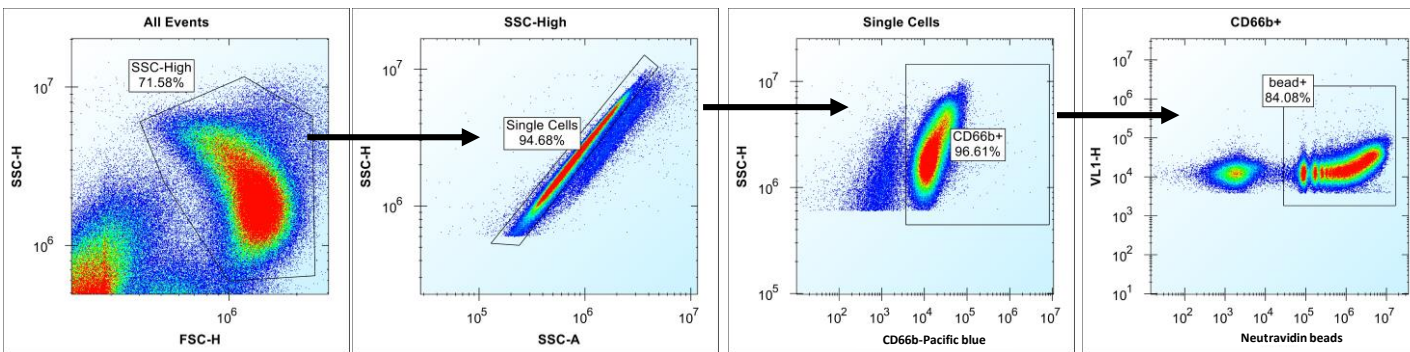
Supplemental Figure 11: The heatmap shows IgG1 (A) and IgM (B) antibody levels against different SARS-CoV-2, common CoVs, other respiratory viruses, KD associated pathogens and MIS-C associated auto-antigens. Values were Z-scored and the average value for each group and antigen was plotted. Some data in this figure has been published elsewhere³(Yonker et.al, *J Pediatr*, 2020). (C) The chord diagrams show the relationships of Luminex defined IgG1 titers across SARS-CoV-2 antigens (upper panel, yellow =RBD, red =S, and blue =N) and other pathogens and auto-antigens (lower panel, yellow = common CoVs RBD, red = other respiratory viruses, blue = KD associated pathogens, green = MIS-C associated auto-antigens) assessed by Spearman correlation. The connecting lines between colored boxes (antigen-specific IgG1 titer) and grey boxes (FcγRs) indicate a significant ($p < 0.05$) correlation between antigen-specific IgG1 titers and binding to the indicated FcγR for the respective antigen. A color-gradient was used to indicate the correlation coefficient (from $r = -1$ (dark blue) over $r = 0$ (white) to $r = 1$ (dark red)) for the individual correlations.



Supplemental Figure 12: Total bulk IgM (A) and IgG (B) ELISA results are shown across plasma from SARS-CoV-2 infected (acute) or uninfected children, as well as children who developed mild or severe MIS-C. Additionally, the IgG-Fc glycosylation was analyzed by capillary electrophoresis. The frequency of IgG-Fc with agalactosylated (G0) (C), galactosylated but not sialylated (D), sialylated (E), fucosylated (F) or bisected (G) N-glycans are shown, respectively.



Supplemental Figure 13: The correlation of Luminex IgG1 and ELISA IgG titers against SARS-CoV-2 RBD (Spearman $r^2=0.53$, $p<0.001$).

A**B****C**

Supplemental Figure 14: The diagram shows the flow cytometry gating strategy for (A) ADCP (corresponding to the data shown in Figure 1C, Figure 4C, Supplemental Figure 4G-I, and Supplemental Figure 10B), (B) HL-60 ADNP (corresponding to the data shown in Figure 1C, Figure 4C, Supplemental Figure 4D-F, Supplemental Figure 5, and Supplemental Figure 10B), and (C) ADNP with primary human neutrophils (corresponding to the data shown in Figure 3A-C).

Supplemental Table 1: Study population demographic and clinical characteristics

	Adult mild COVID (n=34)	Adult severe COVID (n=26)	Adult convalescent (n=18)	pediatric mild COVID (n=25)	pediatric mild MIS-C (n=6)	pediatric severe MIS-C (n=11)
Age, years, median (max, min)	34 (22, 76)	56 (32, 79)	33 (27, 58)	15 (0, 21)	1.8 (0.2, 9.7)	8.3 (1.5, 21.9)
Sex, male, n (%)	15 (44.1)	12 (46.2)	8 (44.4)	15 (60.0)	5 (83)	9 (82)
SARS-CoV-2 serostatus ¹ , n positive (%)	17 (50.0)	26 (100)	18 (100)	13 (52.0)	0 (0)	9 (82)
Days since symptom onset, median (max,min)						
Overall	7 (0, 52)	16 (10, 37)	27 (11, 38)	3 (0, 21)	4.5 (2, 23)	5 (3, 21)
Seropositive	12.5 (2, 41)	16 (10, 37)	27 (11, 38)	7 (0, 21)	-	4.5 (3, 16) ²
Clinical course, n (%)						
hospitalization	0	26 (100)	0	7 (28.0)	6 (100)	11 (100)
ICU treatment	0	15 (57.7)	0	1 (4)	0	7 (64)

¹Sero-status was defined by Luminex assay (see Methods)

² days of MIS-C symptoms

Supplemental Table 2: Demographic, clinical characteristics and diagnostic criteria per CDC case definition of MIS-C patients (CDC: Center for Disease Control)

#	MIS-C severity	Age (years)	Sex	Race/ethnicity	CDC criteria for MIS-C							Disease progression		
					Symptoms	Laboratory evidence of inflammation	Multisystem organ involvement	No alternative plausible diagnosis	One of the following			Hospital level of care	Cardiac involvement	Final Outcome
									SARS-CoV-2 RT-PCR	SARS-CoV-2 antibodies (ELISA)	COVID-19 exposure			
1	mild	0.1	F	unknown	fever, cough, vomiting, diarrhea	(+)	(+)	(+)	(+)	(+)	(+)	ward	none	discharged
2	mild	0.2	M	latino/hispanic	fever, dyspnea	(+)	(+)	(+)	(+)		(+)	ward	none	discharged
3	mild	1.1	M	white	fever, cough	(+)	(+)	(+)			(+)	ward	none	discharged
4	mild	2.5	M	white	fever	(+)	(+)	(+)	(+)		(+)	ward	none	discharged
5	mild	2.9	M	white	fever, rash, vomiting, headache	(+)	(+)	(+)				ward	none	discharged
6	mild	9	M	white	fever, vomiting, diarrhea, myalgia, anosmia	(+)	(+)	(+)		(+)		ward	none	discharged
7	severe	1	M	african american	fever, chills	(+)	(+)	(+)		(+)		ward	coronary dilation	discharged
8	severe	2	F	asian	fever, fatigue	(+)	(+)	(+)	(+)	(+)	(+)	ward	mild pericardial effusion	discharged
9	severe	2.5	M	white	fever, rash, cough, sore throat	(+)	(+)	(+)			(+)	PICU	coronary dilation	discharged
10	severe	3.5	M	latino/hispanic	fever, rash	(+)	(+)	(+)		(+)	(+)	PICU	coronary dilation	discharged
11	severe	7	F	unknown	fever, vomiting, diarrhea	(+)	(+)	(+)	(+)	(+)	(+)	PICU	decreased ventricular function	discharged
12	severe	8.3	M	african american	fever, myalgia	(+)	(+)	(+)		(+)		PICU	ventricular failure: ecmo	discharged
13	severe	10	M	latino/hispanic	fever, rash	(+)	(+)	(+)	(+)	(+)	(+)	PICU	ventricular dilation and dysfunction	discharged
14	severe	12	M	latino/hispanic	fever, rash, dyspnea	(+)	(+)	(+)		(+)	(+)	PICU	coronary dilation, myocarditis	discharged
15	severe	13.5	M	white	fever, chills, headache	(+)	(+)	(+)	(+)	(+)		PICU	myocarditis	discharged
16	severe	19	M	white	fever, chest pain	(+)	(+)	(+)			(+)	PICU	ventricular failure: ecmo	discharged
17	severe	21.9	M	african american-latino/hispanic	fever, anorexia, vomiting, diarrhea	(+)	(+)	(+)		(+)		PICU	ventricular dilation and dysfunction	discharged